

Real-world Instance-specific Image Goal Navigation for Service Robots: Bridging the Domain Gap with Contrastive Learning

Taichi Sakaguchi¹, Akira Taniguchi^{1,*}, Yoshinobu Hagiwara¹, Lotfi El Hafi¹,
Shoichi Hasegawa¹, and Tadahiro Taniguchi¹

Abstract—Improving instance-specific image goal navigation (InstanceImageNav), which locates the identical object in a real-world environment from a query image, is essential for robotic systems to assist users in finding desired objects. The challenge lies in the domain gap between low-quality images observed by the moving robot, characterized by motion blur and low-resolution, and high-quality query images provided by the user. Such domain gaps could significantly reduce the task success rate but have not been the focus of previous work. To address this, we propose a novel method called Few-shot Cross-quality Instance-aware Adaptation (CrossIA), which employs contrastive learning with an instance classifier to align features between massive low- and few high-quality images. This approach effectively reduces the domain gap by bringing the latent representations of cross-quality images closer on an instance basis. Additionally, the system integrates an object image collection with a pre-trained deblurring model to enhance the observed image quality. Our method fine-tunes the SimSiam model, pre-trained on ImageNet, using CrossIA. We evaluated our method’s effectiveness through an InstanceImageNav task with 20 different types of instances, where the robot identifies the same instance in a real-world environment as a high-quality query image. Our experiments showed that our method improves the task success rate by up to three times compared to the baseline, a conventional approach based on SuperGlue. These findings highlight the potential of leveraging contrastive learning and image enhancement techniques to bridge the domain gap and improve object localization in robotic applications. The project website is <https://emergentsystemlabstudent.github.io/DomainBridgingNav/>.

I. INTRODUCTION

In robots assisting users, the ability to accurately locate specific objects, such as a particular can in a domestic setting, is crucial. This challenge is further compounded when multiple instances of the same object class, each with a different appearance, are present within the environment. To successfully execute tasks in such situations, robots need to identify different instances of the same class of objects. One approach to addressing this challenge is **Instance-specific Image Goal Navigation (InstanceImageNav)** [1], which uses a query image. In this task, the robot locates the object

This work was supported by JSPS KAKENHI Grants-in-Aid for Scientific Research (Grant Numbers JP23K16975, 22K12212) and JST Moonshot Research & Development Program (Grant Number JPMJMS2011).

¹Taichi Sakaguchi, Akira Taniguchi, Yoshinobu Hagiwara, Lotfi El Hafi, Shoichi Hasegawa, and Tadahiro Taniguchi are with Ritsumeikan University; 1-1-1 Noji-Higashi, Kusatsu, Shiga 525-8577, Japan. {sakaguchi.taichi, a.taniguchi, yhagiwara, lotfi.elhafi, hasegawa.shoichi, taniguchi}@em.ci.ritsumei.ac.jp

*Corresponding author.

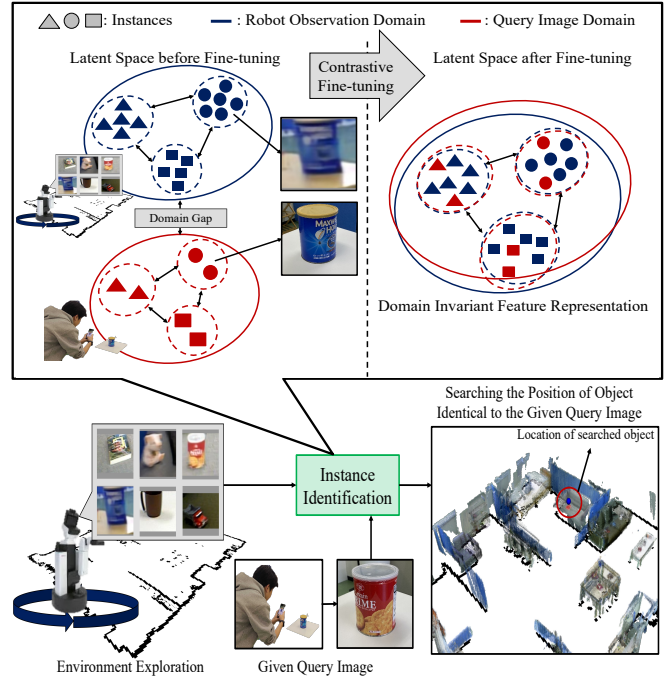


Fig. 1. Focused task in this study. (Bottom) The robot identifies the position of an object shown in a query image provided by a user’s mobile phone. (Top left) Domain gap that the image quality significantly differs between the image taken by the user’s mobile phone and the object image observed by the real robot. (Top right) Contrastive learning to align images of the same instance with different image quality in latent space.

shown in the query image provided by the user’s mobile phone, as shown in Fig. 1 (bottom). If the target instance and other instances can be visually distinguished, the robot can locate an object identical to the provided query image. This highlights that InstanceImageNav is a crucial problem to solve for robots to acquire the ability to search for specific instances in complex real environments.

When robots explore an environment, the images they observe are often of low-quality due to motion blur from movement and low resolution. Low-quality is caused by objects appearing small in the angle of view (see Fig. 2 (top)). This issue is particularly pronounced in data collected by consumer robots used at home, where both the angle of view and image quality may be insufficient. In contrast, query images captured by the user’s mobile phone are typically of high-quality. This **domain gap** in image quality significantly reduces the success rate of InstanceImageNav. Hence, it is important to bridge the domain gap between the robot’s

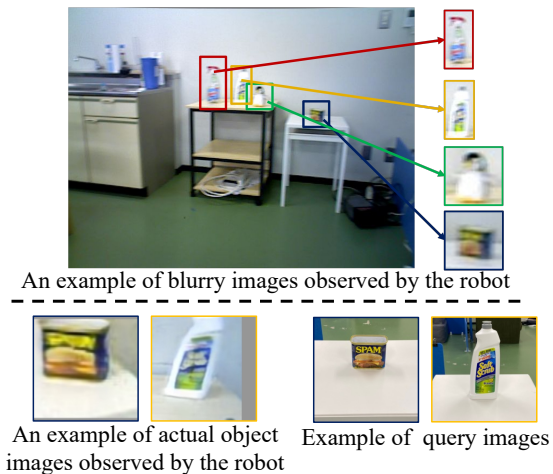


Fig. 2. (Top) Object images cropped from the robot’s observation image; (Bottom left) Examples of low-quality images; (Bottom right) Examples of high-quality images as the query.

observed images and the query images provided by the user, as shown in Fig. 1 (top). To address this challenge, we propose a system that integrates two key mechanisms: one for learning invariant feature representations between low-quality and high-quality images, and another for enhancing the quality of images observed by robots.

To solve InstanceImageNav, prior works proposed navigation systems that combine multiple techniques [2], [3], such as a pre-trained image recognition model and simultaneous localization and mapping (SLAM). For example, Chang *et al.* proposed a system to solve the InstanceImageNav task by exploring the environment and constructing a database that saves 3D semantic maps and images of each instance [3]. They execute the InstanceImageNav by using the technique of local feature matching, SuperGlue [4], to search for the same object as the given query image from the database and identify its position on the 3D semantic map. In addition, in prior works on InstanceImageNav [1], [2], the main evaluation of the proposed method was performed using Habitat Simulator [5]. However, the Habitat simulator does not reproduce phenomena such as motion blur, so domain gaps that occur in the real world are unlikely to be observed.

In previous work on InstanceImageNav [1]–[3], the main search targets are large objects such as “chair”, “desk”, and “television”. However, objects that the user may want the robot to locate include small objects such as “cup”, “bottle”, and “book”. When collecting images of such small objects, the resolution tends to be low, as shown in Fig. 2, and there is a problem that the image quality differs from the query image provided by the user.

To mitigate motion blur, we proposed a system that integrates a pre-trained model for **deblurring** [6] into the object image database construction system similar to the one proposed by Chang *et al.* [3]. Furthermore, it is known that **contrastive learning** enables the acquisition of invariant feature representations between images of the same instance across different domains [7], [8]. Therefore, we propose a

model that **learns invariant feature representations between a few high-quality and massive low-quality images** through contrastive learning with an instance classifier.

In this study, we evaluate the proposed system’s effectiveness in identifying the object identical to the query image from the object images collected by the robot while exploring the real-world environment. In previous work on InstanceImageNav, only one query image is taken for each object [2], [3]. However, images can be captured from various angles by the user. Therefore, we collected eight images for each instance to evaluate the proposed system across various angles of the query object. In this study, the objects for locating are 20 different instances that could be placed on the table. Our main contributions are two-fold.

- 1) We show that contrastive learning with an instance classifier, to learn invariant feature representations between cross-quality images under few-shot conditions, effectively bridging the domain gap that cannot be resolved solely by existing deblurring techniques.
- 2) We show that our system, integrating a data collection module involving 3D semantic mapping, a pre-trained deblurring model, and fine-tuning the SimSiam model, can achieve high accuracy in the InstanceImageNav task.

The remainder of this paper is organized as follows. We provide an overview of related works in Section II. We detail the integration of the proposed method in Section III. We describe our experimental protocols and metrics in Section IV. We present and discuss our results in Section V. Finally, we conclude with directions for future works in Section VI.

II. RELATED WORKS

A. Object Searching

Research on object searching is categorized into three types based on the representation of the searching target. Firstly, Object Goal Navigation (ObjectNav) is the task of locating any object belonging to a given class name such as “book” [9]. Secondly, Vision-and-Language Navigation (VLN) is the task of locating an object represented by language instructions such as “Go to the living room and pick up the yellow cup on the square table.” [10], [11]. Therefore, it is considered that the VLN method also makes it possible to search for specific instances [11]. However, such language instructions require the user to understand where the target object is located within the environment. In the scenario where the user doesn’t know where the desired object is located, the ability to discover the object identical to the query image captured in the past by the user becomes important. Therefore, InstanceImageNav is considered one of the problems to solve to acquire the ability to search for specific instances.

Methods for object searching can be broadly categorized into two types. One is the End-to-End method, which involves learning neural networks that directly generate actions from the robot’s observed images based on deep reinforcement learning or imitation learning [1], [9], [12]. Another

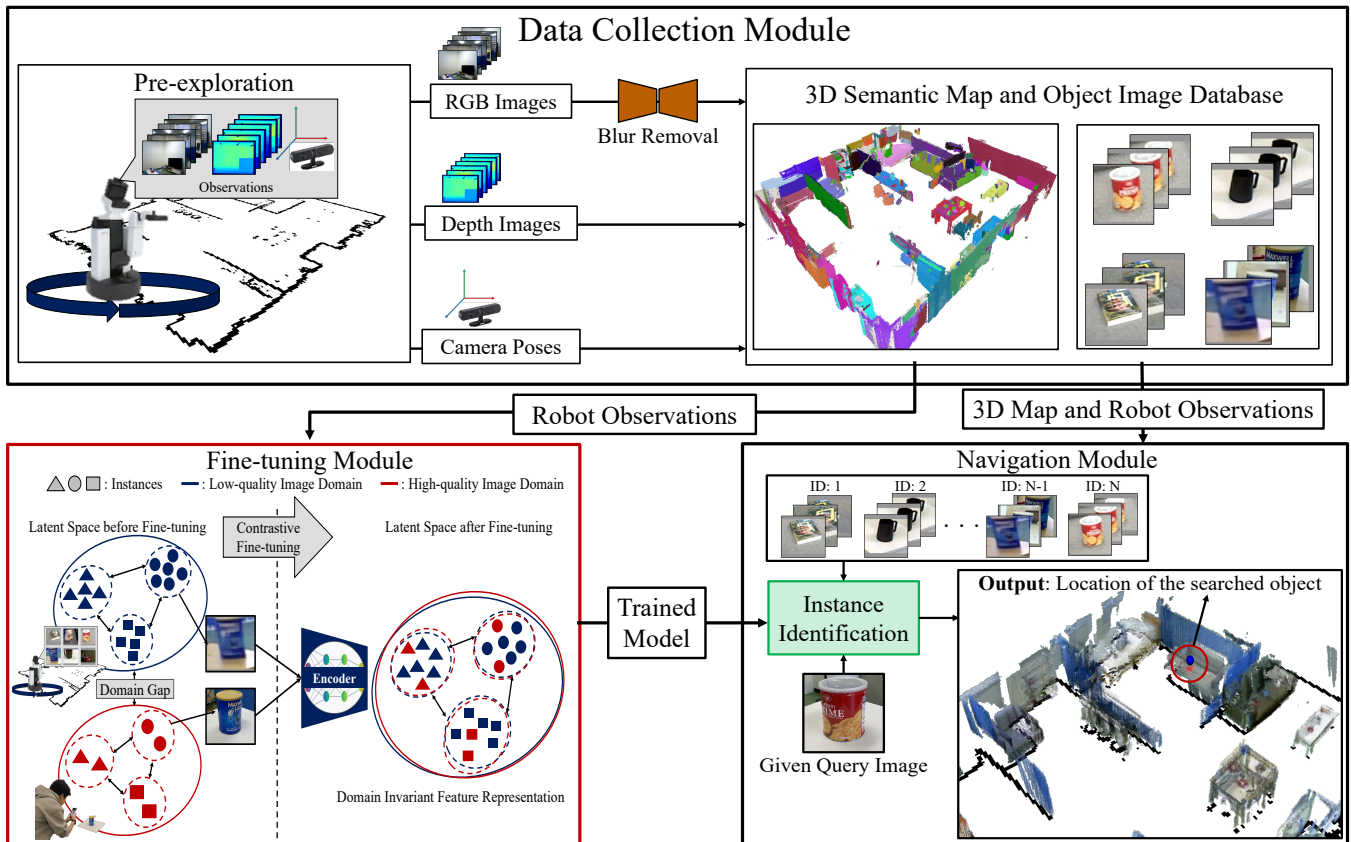


Fig. 3. The overall diagram of the proposed system. The proposed system automatically collects object images from RGBD images and camera pose time series data collected by a robot by exploring the environment in advance. The Fine-tuning Module fine-tunes the pre-trained Image Encoder using the collected object images. The Navigation Module identifies the object’s position identical to the given query image using a fine-tuned image encoder.

is the modular method that integrates components such as object recognition and SLAM [2], [3], [9]. End-to-End method suffer from sample inefficiency [1] and poor sim-to-real transfer [13]. On the other hand, one advantage of the modular method is that it allows tasks to be performed with the same success rate in the real world as in simulation [13]. Therefore, we also propose a modular navigation system.

B. Contrastive Learning

Contrastive learning is a kind of self-supervised learning that involves learning from tasks that contrast different images of the same instance [14]–[17]. Contrastive learning pre-trained models are known to acquire discriminative feature representations that identify different instances belonging to the same class [18]. For example, Ido *et al.* show experimental results showing high accuracy in both instance-level and class-level image classification tasks using features extracted from an image encoder trained via contrastive learning and k-nearest neighbor method [18]. Therefore, models pre-trained by contrastive learning are considered suitable for tasks such as InstanceImageNav, where the objective is to locate the object identical to the query image.

C. Domain-Invariant Feature Learning

In the InstanceImageNav, the images of objects observed by the robot are low-quality, while the provided query im-

ages are high-quality. Thus, learning instance-wise domain-invariant feature representations between high-quality and low-quality images could improve the task’s success rate.

Adversarial learning has been utilized to learn domain-invariant feature representations [19], [20]. This approach enables networks to learn domain-invariant feature representations by back-propagating the reverse gradients of the domain classifier. However, this approach might overlook discrimination between instances.

On the other hand, methods using contrastive learning to obtain domain-invariant feature representations have been proposed [7], [8]. Since contrastive learning enables networks to learn instance discriminative representations [18], approaches based on contrastive learning could learn instance-wise domain-invariant feature representations. Therefore, this study focuses on contrastive learning. An important difference from prior works [7], [8] is that only a few samples for one domain are available in this study.

D. Motion Deblurring

Motion blur occurs when the camera or the subject moves during the sensor’s exposure time, resulting in a blurred image. Therefore, images obtained from sensors of robots moving in the environment for object exploration are likely to be blurred due to motion blur. It is known that motion

blur degrades the recognition accuracy of pre-trained image recognition models [21]. Therefore, navigation systems that search for objects while moving within the environment require mechanisms for deblurring.

The method of deblurring can be broadly categorized into two types. One is formulating the deblurring problem as an optimization problem [22]–[24]. This approach involves optimizing the sharp image and the blur kernel from the blurred image using gradient descent. The other is a learning-based approach. In the learning-based approach, neural networks are trained to restore sharp images from blurred images using pairs of blurred and sharp images [6], [21].

One issue with the approach that formulates the deblurring problem as an optimization problem is the high computational cost, requiring several seconds for deblurring. Therefore, we utilize a learning-based deblurring method [6].

III. PROPOSED SYSTEM

As shown in Fig. 3, the proposed system is divided into three main modules. Firstly, the Data Collection Module constructs the 3D semantic map of the environment and then collects object images. Secondly, the Fine-tuning Module fine-tunes the pre-trained models using the collected object images and few-shot high-quality images provided by the user through contrastive learning. Our contrastive learning is called **Few-shot Cross-quality Instance-aware Adaptation (CrossIA)**. Lastly, the Navigation Module leverages the fine-tuned model and the semantic map to locate objects identical to the query image.

A. Data Collection Module

The Data Collection Module constructs a 3D semantic map from sequence data of RGBD images and camera poses collected by the robot moving in 3D space. The construction of the 3D semantic map involves projecting instance ID information onto a voxel-based 3D map, similar to the method described by Kanechika et al [25]. However, while Kanechika *et al.* construct a 3D semantic map by projecting the class label IDs obtained from semantic segmentation results, we utilize Fast Segment Anything (FastSAM) [26] to construct the 3D semantic map by projecting instance ID information onto the 3D map. To ensure that the constructed 3D map has consistent label IDs from frame to frame, we employ Tateno *et al.*'s method [27] similar to Kanechika *et al.*'s approach [25] for constructing the 3D semantic map.

First, RGB images collected by the robot exploring the environment are inputted into the Multi-Scale Stage Network [6] for deblurring. Next, they are inputted into the FastSAM [26] for image segmentation. Then 3D semantic map is constructed using the segmentation results, depth images, and camera poses.

Next, this module collects object images using a constructed 3D semantic map. During this process, 2D segmentation masks images from the 3D semantic map by ray tracing. Ray tracing generates a mask image from an arbitrary camera pose by sending pseudo-rays in the depth direction from the camera and capturing the instance ID

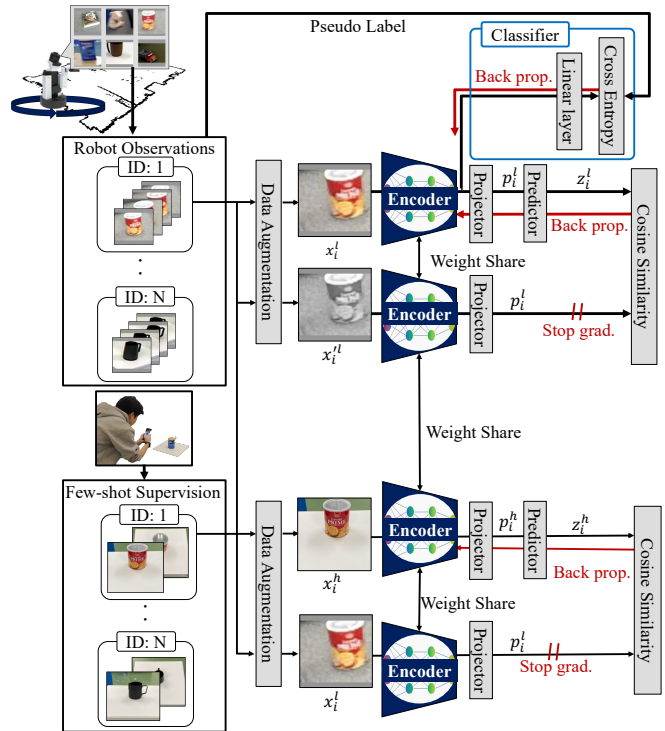


Fig. 4. Overview of the proposed fine-tuning method: Few-shot Cross-quality Instance-aware Adaptation (CrossIA).

of the first collision on the 3D map. This process ensures the consistent generation of pseudo-labels for images of the same instance. Then, the generated mask images are transformed into bounding boxes (BBoxes), and the regions of the transformed BBoxes are extracted from the RGB images to collect object images.

B. Fine-tuning Module

This module fine-tunes a pre-trained image encoder by the contrastive task between low-quality images observed by the robot and few-shot high-quality images provided by the user. SimSiam, a negative free contrastive learning method, is shown to be capable of learning with small batch size [16]. In contrast, contrastive learning methods require negative pairs learning with a huge batch size [14]. Therefore, we utilize SimSiam for fine-tuning.

Additionally, for training, the user needs to capture few-shot images of objects they want the robot to locate with a mobile device and provide them to the robot. This requires the user to instruct the robot, but since it involves only a few images, it could not be considered a significant burden for the user. In this study, we assume that the system has up to five high-quality images for each instance and evaluate the experiments accordingly.

Furthermore, it is shown that by minimizing the loss of contrastive learning and the loss function of the linear classifier for a pre-trained image encoder through fine-tuning, the variance of feature vectors between images of the same label decreases [28]. This characteristic leads to an improvement in the accuracy of image classification tasks.

Therefore, we also conduct fine-tuning of the image encoder by adding a linear classifier to SimSiam as shown in Fig. 4. The label of instances required for calculating the loss of the linear classifier is obtained using pseudo-labels automatically generated by the data collection module. Thus, the loss function during fine-tuning can be represented as follows:

$$\mathcal{L} = \sum_{i=1}^{N_c} \mathcal{L}_i^{cross} + \sum_{i=1}^{N_r} \mathcal{L}_i^{robot}. \quad (1)$$

Loss functions \mathcal{L}_i^{cross} and \mathcal{L}_i^{robot} are calculated as follows:

$$\mathcal{L}_i^{cross} = -\frac{1}{2} \{ \text{CosSim}(p_i^h, z_i^l) + \text{CosSim}(p_i^l, z_i^h) \} + \frac{1}{2} \{ \text{CE}(y_{i,pred}^h, y_{i,true}^h) + \text{CE}(y_{i,pred}^l, y_{i,true}^l) \}, \quad (2)$$

$$\mathcal{L}_i^{robot} = -\frac{1}{2} \{ \text{CosSim}(p_i^l, z_i^l) + \text{CosSim}(p_i^l, z_i^l) \}, \quad (3)$$

where $\text{CE}()$ and $\text{CosSim}()$ denote cross-entropy and cosine similarity. p_i^l and z_i^l are the outputs of SimSiam’s projector and predictor of the object image x_i^l observed by the robot, respectively. p_i^l and z_i^l are the outputs of SimSiam’s projector and predictor of the object image x_i^l where x_i^l and x_i^l are different images of the same object generated by data augmentation. $y_{i,pred}^l$ is the prediction result when x_i^l is classified. p_i^h and z_i^h are the outputs of projector and predictor, respectively, when the high-quality image x_i^h is input to SimSiam, and $y_{i,pred}^h$ is the prediction result when x_i^h is classified.

Therefore, fine-tuning the image encoder involves contrastive learning between high-quality and low-quality images, and the contrastive learning between images the robot observed. In this paper, $\{(x_i^l, x_i^h, y_{i,true})\}_{i=1}^{N_c}$ is the set of high-quality image, low-quality image and their label and $\{(x_i^l, y_{i,true})\}_{i=1}^{N_r}$ is the set of images and their labels of low-quality image.

C. Navigation Module

As illustrated in Fig. 3, the Navigation Module locates the object identical to the given query image. This is conducted by leveraging images of objects collected by the Data Collection Module, the 3D semantic map, and feature vectors extracted from the fine-tuned image encoder.

First, the fine-tuned image encoder is utilized to compute the feature vectors x_{obs} and x_{query} for the object images collected by the Data Collection Module and the query image, respectively. Using these feature vectors, the similarity s between the query image and the observed object images is calculated using the cosine similarity shown as follows:

$$\text{CosSim}(x_{query}, x_{obs}) = \frac{x_{query}}{\|x_{query}\|_2} \cdot \frac{x_{obs}}{\|x_{obs}\|_2}. \quad (4)$$

Then, the instance with the highest similarity to the query image is identified.

Next, the module identifies the centroid coordinates of the object on the 3D map that is most similar to the query image, and the robot moves to close it. The centroid coordinates of the object are determined by computing the average of the 3D

coordinates of the voxels with the same ID as the identified instance. Upon determining the centroid coordinates of the object as the target point, if the occupied position on the map is designated as the target point, it may result in failed navigation. Therefore, to overcome this issue, the module selects unoccupied regions within a radius of 1.0 [m] from the object’s centroid as the target point for navigation. The value of 1.0 [m] is chosen based on Krantz *et al.*’s definition of success criteria for the InstanceImageNav task, where the distance between the target object and the robot is defined as 1.0 [m] or less.

IV. EXPERIMENTS

If our proposed system can accurately identify the object identical to the query image within observed images using the navigation module, moving to the target object would be possible. Therefore, in this experiment, we evaluate the proposed system by identifying the object identical to the query image from the observed images. The purpose of this experiment is two-fold.

- 1) We verify whether introducing deblurring during exploring in the environment can improve the success rate of the task.
- 2) We verify whether fine-tuning a pre-trained model using contrastive learning with images observed by the robot and a few-shot high-quality images provided by the user can improve the success rates in the task.

A. Comparison methods

In this experiment, we compare SuperGlue [4], which is utilized in prior works of InstanceImageNav [2], [3], image encoder pre-trained by SimSiam [16], and the proposed CrossIA. The baselines for this experiment are the condition where models pre-trained on open dataset [29], [30] are utilized without utilizing a deblurring method to identify the object identical to the query image. In addition, we evaluated a method to learn domain-invariant feature representations by combining contrastive learning and adversarial learning with domain labels [19]. It is expected that domain-invariant feature representation can be learned even when the amount of high-quality images provided during training is small.

B. Conditions and Dataset

The data collected in this experiment were obtained using the Human Support Robot [31] built by Toyota Motor Corporation. Additionally, the RGBD sensor attached to HSR is the Asus Xtion Pro Live. This camera can capture RGB images with a resolution of 640×480 at 30 fps. The RGBD sensor is mounted about 1 [m] above the ground.

During data collection, the robot was moved throughout the environment without stopping in front of specific objects, and the entire 74 [m²] area was scanned in 2 minutes to construct a 3D semantic map. This exploration collected 606 RGBD images. The constructed dataset contains 145 instances, and 2011 images were collected in total.

In InstanceImageNav proposed by Krantz *et al.* [1], the instances for locating are objects belonging to classes of

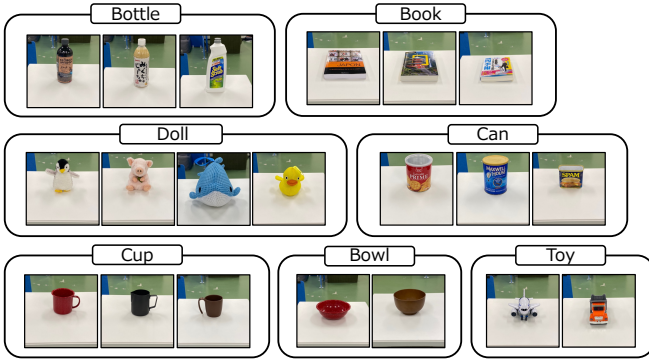


Fig. 5. The instances targeted for search in this experiment.

large objects such as “Chair”, “Table”, “TV”. However, users could request to discover small objects, such as those that can be placed on a table. Therefore, in this experiment, the instances for locating are instances belonging to the classes of “Bottle”, “Cup”, “Can”, “Bowl”, “Doll”, or “Toy”, as shown in Fig. 5.

The query images for each instance were taken using the camera of an iPhone 11 Pro. When capturing the query images, the photographer took the pictures from a distance of 40 [cm]. Moreover, in studies addressing the InstanceImageNav task in the real world, only one image is captured for each instance. However, query images taken by users may be captured from various angles. Therefore, in this experiment, when capturing the query images, the photographer took pictures from eight different directions, standing and crouching, to prepare 32 types of query images for each instance.

C. Evaluation Metrics

The evaluation metrics for the task include the success rate (SR), the mean reciprocal rank (MRR) [32], and the mean rank (MR). SR is used to evaluate the accuracy of identifying the object identical to the query image as the top-ranked item among the observed object images by the robot. MRR is a metric that evaluates how well the object identical to the query image can be identified at higher ranks. In Eq. (5), s_n represents a binary variable indicating whether the task was successful for each instance, where $s_n = 1$ if the query image task was successful and $s_n = 0$ otherwise:

$$\text{SR} = \frac{1}{N} \sum_{n=1}^N s_n, \quad (5)$$

$$\text{MRR} = \frac{1}{N} \sum_{n=1}^N \frac{1}{k_n}, \quad (6)$$

where N is the number of trials, which in this study $N = 640$ since a total of 640 query images were collected. k_n is the rank at which the same object as the query image is retrieved.

MR is the reciprocal of MRR and is a metric that indicates the rank in which the same object as the query image was searched for on average across all trials of the task.

TABLE I
SCORE RESULTS OF COMPARISON METHODS

Methods	Deblurring	SR \uparrow	MRR \uparrow	MR \downarrow
SuperGlue	—	0.23	0.32	3.1
SuperGlue	✓	0.23	0.34	3.0
SimSiam	—	0.30	0.41	2.4
SimSiam	✓	0.33	<u>0.43</u>	2.3
CrossIA (Ours)	✓	0.70	0.78	1.3
CrossIA with [19]	✓	<u>0.68</u>	0.78	1.3

TABLE II
SCORES OF FINE-TUNED SIMSIAM BASED ON FEW-SHOT CONDITIONS

Methods	SR \uparrow	MRR \uparrow	MR \downarrow
One-shot	0.35 (0.45)	0.48 (0.59)	2.1 (1.7)
Three-shot	0.62 (0.61)	0.71 (0.69)	1.4 (1.4)
Five-shot	0.70 (0.68)	0.78 (0.78)	1.3 (1.3)

The numbers in parentheses are the results with the addition of adversarial learning [19].

V. RESULTS

Table I shows the metrics scores under the conditions written in the table. Firstly, when we compare the evaluation index scores of the baseline method of this experiment and the method proposed in this study, we find that the SR score has improved by 3 times and the MRR score has improved by 2.4 times. In addition, the baseline method searches for the same object as the query image in third place on average across all task trials, but the proposed method in this study can search for the same object in first place on average. In addition, when comparing the metrics scores under the condition of using SimSiam with only pre-training on ImageNet, which is used in the method proposed in this research, the SR score improves by 2.3 times and the MRR score improves by 1.8 times. Furthermore, adding adversarial learning did not result in significant improvements compared to methods that only use contrastive learning.

Secondly, when comparing the metrics scores with and without blur removal under the conditions of the pre-trained model, it is found that there is no significant difference under any of the conditions of SuperGlue [4] and SimSiam [16]. This suggests that learning domain-invariant feature representations contributes more to improving the task success rate than removing blur from the robot’s observed images.

Lastly, we compare the distribution of the query image and the object image observed by the robot in the latent space using the SimSiam, which was only pre-trained on ImageNet, and the SimSiam fine-tuned by our method. As shown in Fig. 6(a), in the latent space of the SimSiam, which was only pre-training on ImageNet, high-quality and low-quality images were separated in the latent space. On the other hand, as shown in Fig. 6(c) in the latent space of the SimSiam, which was fine-tuned by the proposed method, data of the same instance with different domains are distributed close to each other. In addition, as shown in Fig. 6(b) in the latent space of the SimSiam, which was fine-tuned with only images observed by the robot, the observed images of the same instance are close to each other.

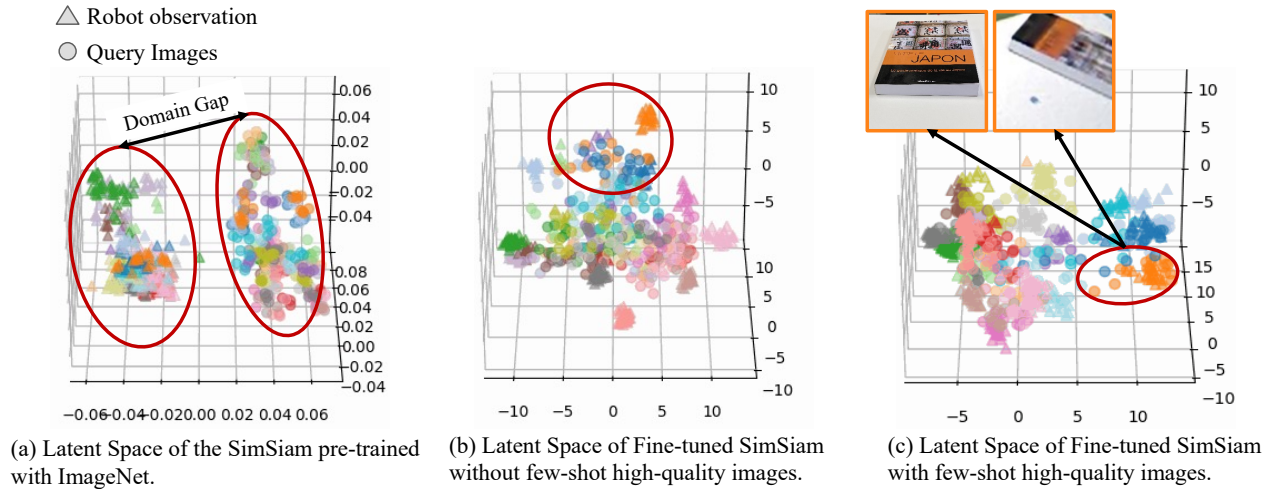


Fig. 6. Latent Spaces of SimSiam for different training conditions. (a) The data between different domains are spatially separated. (b) Only low-quality images of the same instance are closer, as shown in the region marked by the red ellipse. (c) Images from different domains of the same instance become closer in the latent space.

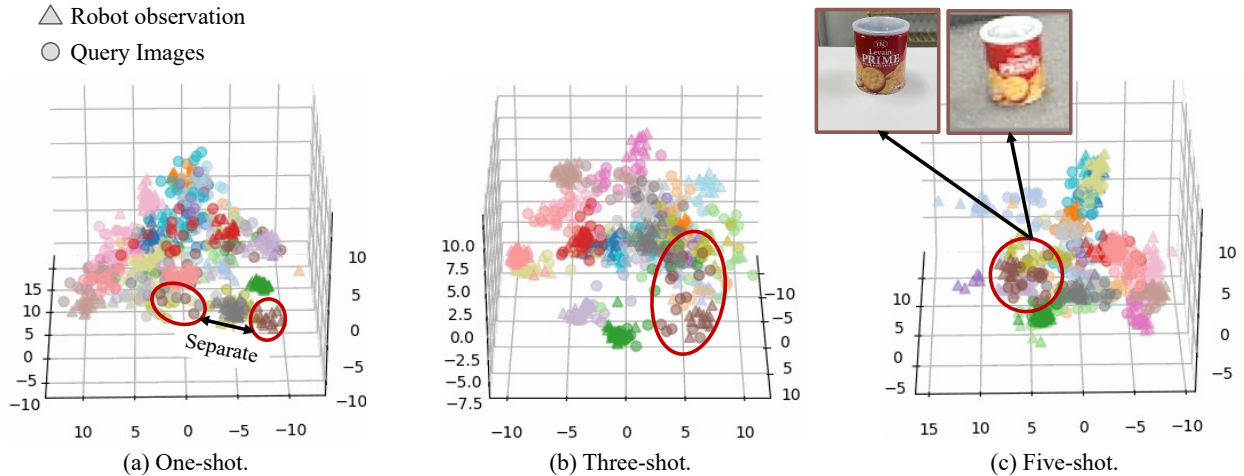


Fig. 7. Comparison of latent spaces acquired in different training conditions that the model trained with robot observation and few-shot high-quality images. As shown by the red ellipse in each figure, the smaller the number of high-quality images given during training, the further separate the images between different domains become in the latent space.

However, it can be seen that the query images, which is a high-quality image, separate. These results suggest that contrastive learning between the same instance images of different domains, as in the method proposed in this study, contributes to improving the success rate of the task.

To verify how small the number of high-quality images provided when fine-tuning is performed by the proposed method, the improvement in the task success rate decreases, we examined the high-quality images provided for each object to be searched. Table II shows the metrics scores under conditions where the number of high-quality images given during learning was changed. The success rate of the task decreases as the number of given high-quality images during training decreases. As shown in Fig. 7, images from different domains tend to become closer in latent space as the number of high-quality images provided during training

increases. This result suggests that providing adequate high-quality images during training enhances the ability to obtain domain-invariant feature representations through contrastive learning.

In under one-shot conditions, when adversarial learning was added, the scores of all evaluation metrics were improved compared to only contrastive learning. This result suggests that multi-task learning of adversarial learning and contrastive learning could make images of different domains closer in the latent space even with fewer high-quality images than only contrastive learning.

VI. CONCLUSION

We proposed a method to solve the problem that the success rate of InstanceImageNav degrades due to the domain gap in image quality between the image observed by the

robot and the image provided by the user utilizing few-shot high-quality images and robot observations. Specifically, we proposed a method, CrossIA, that uses contrastive learning to learn domain-invariant feature representations between images observed by the robot and high-quality few-shot images. We compared the proposed method with the baseline method through experiments. The experiment results showed that the task’s success rate was improved threefold compared to the baseline method.

The method proposed in this research assumes that the user provides a few high-quality images. The number of images provided for each object is small. Still, as the number of objects to be searched increases, the number of images that need to be provided also increases. Therefore, we consider that a method that does not require the user to provide high-quality images for training is necessary.

As one of the developments of the proposed method, developing a method to bridge the domain gap between high-quality images and low-quality images without requiring the user to provide the high-quality image necessary for training is essential. One way to do this is to use an image restoration method with a pre-trained diffusion model [33]. Applying the image restoration method during data augmentation allows for automatically generating high-quality images from low-quality images observed by a robot. Therefore, in the future, we will verify whether the task’s success rate improves similarly when using images automatically generated using image restoration methods and images observed by a robot.

REFERENCES

- [1] J. Krantz, S. Lee, J. Malik, D. Batra, and D. S. Chaplot, “Instance-Specific Image Goal Navigation: Training Embodied Agents to Find Object Instances,” *arXiv preprint arXiv:2211.15876*, 2022.
- [2] J. Krantz, T. Gervet, K. Yadav, A. Wang, C. Paxton, et al., “Navigating to Objects Specified by Images,” in *IEEE/CVF International Conference on Computer Vision (ICCV)*, 2023, pp. 10916–10925.
- [3] M. Chang, T. Gervet, M. Khanna, S. Yenamandra, D. Shah, et al., “GOAT: Go to Any Thing,” *arXiv preprint arXiv:2311.06430*, 2023.
- [4] P.-E. Sarlin, D. DeTone, T. Malisiewicz, and A. Rabinovich, “SuperGlue: Learning Feature Matching with Graph Neural Networks,” in *IEEE/CVF Computer Vision and Pattern Recognition Conference (CVPR)*, 2020, pp. 4938–4947.
- [5] M. Savva, A. Kadian, O. Maksymets, Y. Zhao, E. Wijmans, et al., “Habitat: A Platform for Embodied AI Research,” in *IEEE/CVF International Conference on Computer Vision (ICCV)*, 2019, pp. 9339–9347.
- [6] K. Kim, S. Lee, and S. Cho, “MSSNet: Multi-Scale-Stage Network for Single Image Deblurring,” in *European Conference on Computer Vision (ECCV)*, 2022, pp. 524–539.
- [7] R. Wang, Z. Wu, Z. Weng, J. Chen, G.-J. Qi, et al., “Cross-domain Contrastive Learning for Unsupervised Domain Adaptation,” *IEEE Transactions on Multimedia*, 2022.
- [8] A. Singh, “CLDA: Contrastive Learning for Semi-Supervised Domain Adaptation,” *Advances in Neural Information Processing Systems (NeurIPS)*, vol. 34, pp. 5089–5101, 2021.
- [9] B. Li, J. Han, Y. Cheng, C. Tan, P. Qi, et al., “Object Goal Navigation in Embodied AI: A Survey,” in *International Conference on Video, Signal and Image Processing (VSIP)*, 2022, pp. 87–92.
- [10] J. Gu, E. Stefani, Q. Wu, J. Thomason, and X. Wang, “Vision-and-Language Navigation: A Survey of Tasks, Methods, and Future Directions,” *Association for Computational Linguistics (ACL)*, pp. 7606–7623, 2022.
- [11] K. Kaneda, S. Nagashima, R. Korekata, M. Kambara, and K. Sugiura, “Learning-To-Rank Approach for Identifying Everyday Objects Using a Physical-World Search Engine,” *IEEE Robotics and Automation Letters*, 2024.
- [12] K. Yadav, R. Ramrakhya, A. Majumdar, V.-P. Berges, S. Kuhar, et al., “Offline Visual Representation Learning for Embodied Navigation,” in *Workshop on Reincarnating Reinforcement Learning at International Conference on Learning Representations (ICLR)*, 2023.
- [13] T. Gervet, S. Chintala, D. Batra, J. Malik, and D. S. Chaplot, “Navigating to Objects in the Real World,” *Science Robotics*, vol. 8, no. 79, p. eadf6991, 2023.
- [14] T. Chen, S. Kornblith, M. Norouzi, and G. Hinton, “A Simple Framework for Contrastive Learning of Visual Representations,” in *International Conference on Machine Learning (ICML)*, 2020, pp. 1597–1607.
- [15] K. He, H. Fan, Y. Wu, S. Xie, and R. Girshick, “Momentum Contrast for Unsupervised Visual Representation Learning,” in *IEEE/CVF Computer Vision and Pattern Recognition Conference (CVPR)*, 2020, pp. 9729–9738.
- [16] X. Chen and K. He, “Exploring Simple siamese Representation Learning,” in *IEEE/CVF Computer Vision and Pattern Recognition Conference (CVPR)*, 2021, pp. 15750–15758.
- [17] J.-B. Grill, F. Strub, F. Altché, C. Tallec, P. H. Richemond, et al., “Bootstrap Your Own Latent: A New Approach to Self-Supervised Learning,” in *Advances in Neural Information Processing Systems (NeurIPS)*, vol. 33, 2020, pp. 21271–21284.
- [18] I. Ben-Shaul, R. Shwartz-Ziv, T. Galanti, S. Dekel, and Y. LeCun, “Reverse Engineering Self-Supervised Learning,” *Advances in Neural Information Processing Systems (NeurIPS)*, vol. 37, 2023.
- [19] Y. Ganin, E. Ustinova, H. Ajakan, P. Germain, H. Larochelle, et al., “Domain-Adversarial Training of Neural Networks,” *Journal of machine learning research*, vol. 17, no. 59, pp. 1–35, 2016.
- [20] E. Tzeng, J. Hoffman, K. Saenko, and T. Darrell, “Adversarial discriminative domain adaptation,” in *IEEE/CVF Computer Vision and Pattern Recognition Conference (CVPR)*.
- [21] O. Kupyn, V. Budzan, M. Mykhailych, D. Mishkin, and J. Matas, “DeblurGAN: Blind Motion Deblurring Using Conditional Adversarial Networks,” in *IEEE/CVF Computer Vision and Pattern Recognition Conference (CVPR)*, 2018, pp. 8183–8192.
- [22] S. Cho and S. Lee, “Fast Motion Deblurring,” in *ACM Transactions on Graphics (SIGGRAPH Asia)*, 2009, pp. 1–8.
- [23] Q. Shan, J. Jia, and A. Agarwala, “High-Quality Motion Deblurring from a Single Image,” *ACM Transactions on Graphics (SIGGRAPH)*, vol. 27, no. 3, pp. 1–10, 2008.
- [24] D. Ren, K. Zhang, Q. Wang, Q. Hu, and W. Zuo, “Neural Blind Deconvolution using Deep Priors,” in *IEEE/CVF Computer Vision and Pattern Recognition Conference (CVPR)*, 2020, pp. 3341–3350.
- [25] A. Kanechika, L. El Hafi, A. Taniguchi, Y. Hagiwara, and T. Taniguchi, “Interactive Learning System for 3D Semantic Segmentation with Autonomous Mobile Robots,” in *IEEE/SICE International Symposium on System Integration (SII)*, 2024, pp. 1274–1281.
- [26] X. Zhao, W. Ding, Y. An, Y. Du, T. Yu, et al., “Fast Segment Anything,” *arXiv preprint arXiv:2306.12156*, 2023.
- [27] K. Tateno, F. Tombari, and N. Navab, “Real-time and Scalable Incremental Segmentation on Dense SLAM,” in *IEEE/RSJ International Conference on Intelligent Robots and Systems (IROS)*, 2015, pp. 4465–4472.
- [28] Y. Zhang, B. Hooi, D. Hu, J. Liang, and J. Feng, “Unleashing the Power of Contrastive Self-Supervised Visual Models via Contrast-Regularized Fine-Tuning,” *Advances in Neural Information Processing Systems (NeurIPS)*, vol. 34, pp. 29848–29860, 2021.
- [29] A. Dai, A. X. Chang, M. Savva, M. Halber, T. Funkhouser, et al., “ScanNet: Richly-annotated 3D Reconstructions of Indoor Scenes,” in *IEEE/CVF Computer Vision and Pattern Recognition Conference (CVPR)*, 2017, pp. 5828–5839.
- [30] J. Deng, W. Dong, R. Socher, L.-J. Li, K. Li, et al., “ImageNet: A Large-Scale Hierarchical Image Database,” in *IEEE/CVF Computer Vision and Pattern Recognition Conference (CVPR)*, 2009, pp. 248–255.
- [31] T. Yamamoto, K. Terada, A. Ochiai, F. Saito, Y. Asahara, et al., “Development of Human Support Robot as the Research Platform of a Domestic Mobile Manipulator,” *ROBOMECH Journal*, vol. 6, 2019.
- [32] T.-Y. Liu, “Learning to Rank for Information Retrieval,” *Foundations and Trends in Information Retrieval*, vol. 3, no. 3, pp. 225–331, 2009.
- [33] X. Lin, J. He, Z. Chen, Z. Lyu, B. Fei, et al., “Diffbir: Towards blind image restoration with generative diffusion prior,” *arXiv preprint arXiv:2308.15070*, 2023.